

[CASE REPORT]

Sonographic Multifocal Cranial Nerve Enlargement in Multifocal Acquired Demyelinating Sensory and Motor Neuropathy

Yuwa Oka^{1,3}, Kazuto Tsukita^{1,4,5}, Koji Tsuzaki^{1,2}, Naoko Takamatsu^{1,6} and Toshiaki Hamano^{1,2}

Abstract:

Multifocal enlargements with the alteration of a normal fascicular pattern are considered to be sonographic peripheral nerve features in multifocal acquired demyelinating sensory and motor neuropathy (MADSAM), a subtype of chronic inflammatory demyelinating polyradiculoneuropathy (CIDP). We herein present the case of an 18-year-old patient with MADSAM in whom intensive sonological assessments revealed multifocal nerve enlargement within clinically affected cranial nerves. Our case demonstrated that, if systematically investigated with ultrasound, morphological changes similar to those in the peripheral nerves may be detected in a large proportion of clinically affected cranial nerves in MADSAM, boosting the future applications of cranial nerve ultrasound in CIDP.

Key words: diagnostic imaging, ultrasonography, ultrasound, chronic inflammatory demyelinating polyneuropathy, CIDP, MADSAM

(Intern Med 60: 2867-2871, 2021)

(DOI: 10.2169/internalmedicine.6782-20)

Introduction

Multifocal acquired demyelinating sensory and motor neuropathy (MADSAM), also known as Lewis-Sumner syndrome or multifocal chronic inflammatory demyelinating polyradiculoneuropathy (CIDP), is a subtype of CIDP. MADSAM presents with chronic sensorimotor multiple mononeuropathy and is characterized by the presence of multifocal sensorimotor conduction blocks (CBs) in nerve conduction studies (NCSs) (1, 2). While the symptoms of MADSAM are usually confined to the peripheral nerves, they can accompany cranial nerve involvement in 17-48% of patients (2-4).

Recently, peripheral nerve ultrasound has become a commonly used clinical tool to complement electrophysiological studies (5-7). Multifocal enlargements with the alteration of a normal fascicular pattern, especially those at the site of

sensorimotor CBs, are considered to be sonographic morphological features of the peripheral nerve in MADSAM (8-11). However, reports on the sonographic investigation of the cranial nerve, especially apart from the vagus nerve (12), remains scarce in the relevant literature, which hampers the clinical application of cranial nerve ultrasound. We herein report a rare case of an 18-year-old patient with MADSAM, in whom intensive sonographic assessments of the cranial nerves revealed multifocal nerve enlargement within clinically affected cranial nerves, suggesting the potential of cranial nerve ultrasound to sensitively disclose morphological changes in MADSAM.

Methods

All NCSs were performed with a Neuropack MEB-2200 (Nihon Kohden, Japan), according to an established protocol (13, 14). Short segment NCSs were also performed to precisely localize CBs. Ultrasound was performed by experi-

¹Department of Neurology, Kansai Electric Power Hospital, Japan, ²Division of Clinical Neurology, Kansai Electric Power Medical Research Institute, Japan, ³Department of Neurology, Kitano Hospital, Tazuke Kofukai Medical Research Institute, Japan, ⁴Department of Neurology, Graduate School of Medicine, Kyoto University, Japan, ⁵Laboratory of Barriology and Cell Biology, Graduate School of Frontier Biosciences, Osaka University, Japan and ⁶Department of Neurology, Tokushima University, Japan

Received: December 18, 2020; Accepted: February 1, 2021; Advance Publication by J-STAGE: March 22, 2021

Correspondence to Dr. Kazuto Tsukita, kazusan@kuhp.kyoto-u.ac.jp

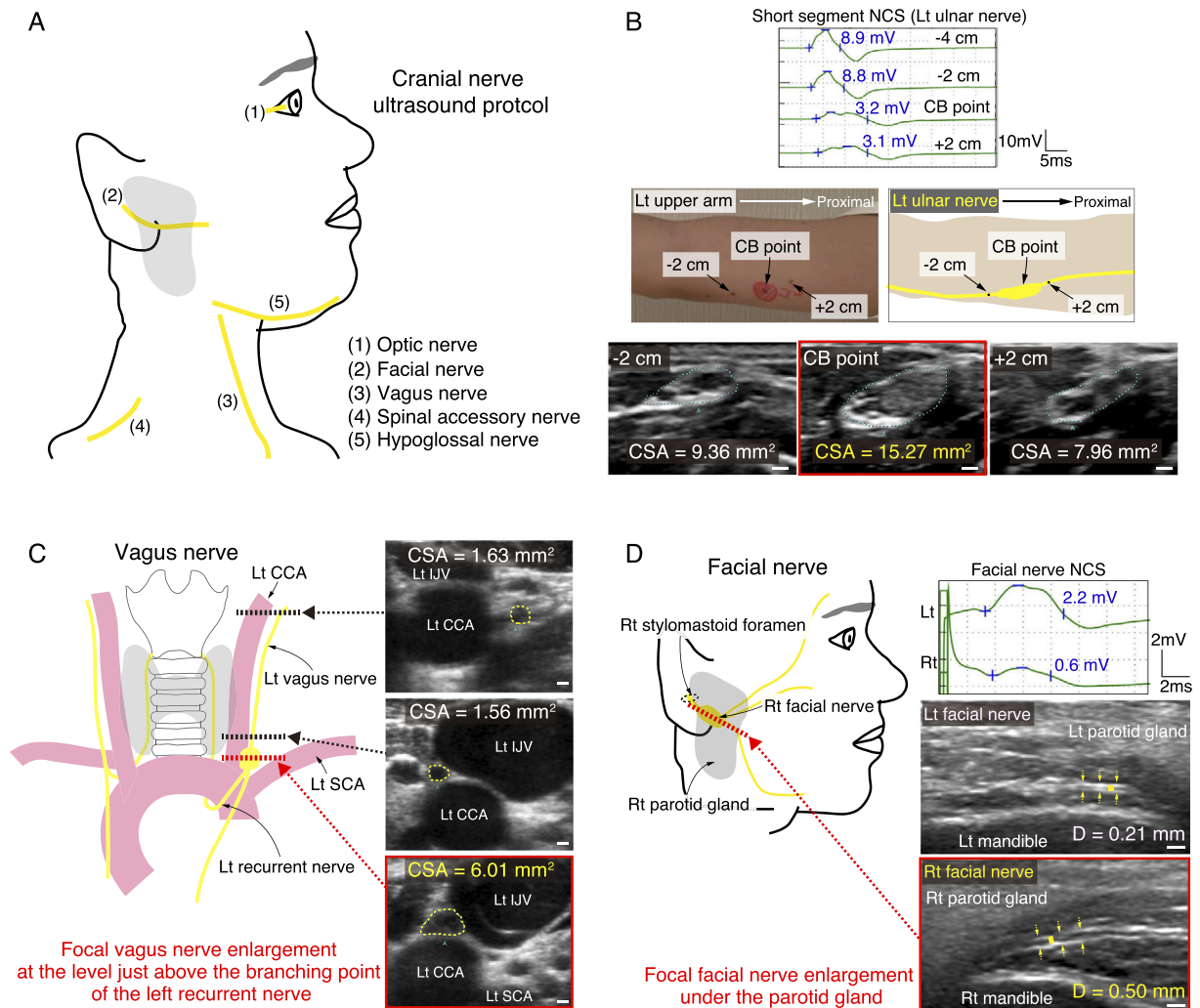


Figure. (A) A schematic drawing showing the examined portion of the cranial nerve in our cranial nerve ultrasound protocol. (B) Representative nerve conduction study (NCS) results and sonographic images of the left ulnar nerve. Note that the left ulnar nerve became focally enlarged in the upper arm at the site of the conduction block. (C) A representative schematic drawing and sonographic images of the left vagus nerve. Note that the left vagus nerve became focally enlarged at the level just above the branching point of the left recurrent nerve. (D) A Representative NCS results and sonographic images of the facial nerve. Scale bars, 1 mm. CCA: common carotid artery, CSA: cross-sectional area, D: diameter, Lt: left, Rt: right, SCA: subclavian artery

enced neurosonographers (KaT and NT: registered neurosonographers of the Japan Academy of Neurosonology) using an ultrasound system (Aplio500, Toshiba, Tokyo, Japan) equipped with a 12 MHz linear-array transducer. We routinely measured cross-sectional areas (CSAs) of the bilateral median nerves, ulnar nerves, and cervical nerve roots (C5-C7) at standardized points by tracing inside the hyperechoic rim of the nerve using a direct tracing method. These values were then analyzed in reference to normal values that were determined in previous studies (15, 16). We also conducted an ultrasonological “inching” study to determine morphological changes of the peripheral nerve at the site of CBs (11). In addition, we conducted systematic sonographic assessments of cranial nerves involving the bilateral hypoglossal, spinal accessory, cervical vagus, and facial

nerves (17-20) (Figure A). We scanned as far along the lengths of these cranial nerves as possible; when focal enlargement or prominent right-to-left differences were noted, we measured the CSAs or diameters, as appropriate (17-21). Described in greater detail below, we measured the left vagus nerve CSA at the level just above the branching point of the recurrent nerve and the bilateral facial nerve diameters under the parotid gland after its emergence from the stylo-mastoid foramen. These measurements were compared to the values obtained from 10 sex-matched normal controls (NCs) [age, 18 years (patient) vs. 30.3±3.7 years (NCs); height, 158 (patient) vs. 172.3±6.5 cm (NCs); weight 45.3 (patient) vs. 63.4±2.5 kg (NCs); BMI, 18.1 (patient) vs. 21.3±2.5 (NCs)]; therefore, when interpreting our results, it should be taken into account that the patient was relatively

Table 1. Results of Motor Nerve Conduction Studies.

Nerve and site	Latency (ms) (upper limits)	CMAP amplitude (mV) (lower limits)	CMAP duration (ms) (upper limits)	Conduction velocity (m/s) (lower limits)	F-wave latency (ms) (upper limits)	F-wave occurrence (%)
Rt median nerve						
Wrist	2.6 (<4.2)	12.0 (>3.5)	5.1 (<6.6)	-	<u>42.7</u> (<31)	100
Elbow	13.1 (<8.8)	<u>5.7 (CB)</u> (>3.5)	8.8	<u>28.6</u> (Wrist-Elbow) (>38)	-	-
Axilla	16.2 (<11.6)	6.1 (>3.5)	7.9	<u>32.8</u> (Elbow-Axilla) (>48)	-	-
Lt median nerve						
Wrist	2.7 (<4.2)	13.8 (>3.5)	6.2 (<6.6)	-	<u>37.3</u> (<31)	81
Elbow	6.8 (<8.8)	13.0 (>3.5)	6.1	50.6 (Wrist-Elbow) (>38)	-	-
Axilla	7.9 (<11.6)	13.0 (>3.5)	6.4	66.7 (Elbow-Axilla) (>48)	-	-
Rt ulnar nerve						
Wrist	2.7 (<3.4)	10.2 (>2.8)	6.6 (<6.7)	-	25.7 (<32)	100
Below elbow	6.1 (<7.5)	10.0 (>2.7)	7.1	59.5 (Wrist-below Elbow) (>49)	-	-
Above elbow	7.1 (<9.6)	9.6 (>2.7)	7.1	53.9 (Below-Above elbow) (>50)	-	-
Axilla	8.0 (<11.7)	10.2 (>2.7)	6.8	60.5 (Above elbow-Axilla) (>54)	-	-
Lt ulnar nerve						
Wrist	3.1 (<3.4)	9.8 (>2.8)	<u>7.0</u> (<6.7)	-	<u>33.7</u> (<32)	100
Below elbow	6.7 (<7.5)	8.9 (>2.7)	7.4	55.6 (Wrist-below Elbow) (>49)	-	-
Above elbow	8.1 (<9.6)	8.4 (>2.7)	7.6	50.5 (Below-Above elbow) (>50)	-	-
Axilla	9.0 (<11.7)	<u>3.0 (CB)</u> (>2.7)	10.2	53.2 (Above elbow-Axilla) (>54)	-	-

Values were presented with upper or lower limits, as appropriate (13, 14). Abnormal values are underlined. The amplitude of compound muscle action potential (CMAP) was measured from baseline to peak. Rt: right, Lt: left, CB: conduction block

younger, thinner, and smaller than the NCs. Values obtained from NCs were presented as the mean±standard deviation.

Case Report

A previously healthy 18-year-old man with no history of preceding infection and no family history of peripheral neuropathy was admitted to our institute with right facial weakness, right-hand weakness, and right-hand hypoesthesia, which gradually progressed over two weeks. He also had a history of left ulnar neuropathy one year previously and left recurrent laryngeal neuropathy 6 months previously, both of which resolved completely with intravenous prednisolone.

A neurological examination revealed difficulties in closing the right eye, raising the right eyebrow, and lifting the right corner of the mouth. There was weakness (manual muscle testing of 3-4 according to the Medical Research Council system) without associated atrophy, in the right abductor pollicis brevis, first dorsal interosseous, and abductor digiti minimi. The deep tendon reflexes of the biceps brachii, brachioradialis, and triceps brachii were normal bilaterally. The right thumb, index, ring, and little fingers demonstrated decreased sensation to light touch and pinprick. These findings suggested right facial, median, and ulnar neuropathies.

Motor NCS revealed CBs in the right median nerve between the elbow and axilla and in the left ulnar nerve between the elbow and axilla (Table 1). Additionally, other demyelinating electrophysiological features, including the prolongation of F-wave latency, were observed asymmetrically in the median and ulnar nerves (Table 1). Sensory NCS did

not reveal any abnormalities at the distal end of the investigated nerves, and there were no abnormal median-normal sural sensory responses (22). Next, a short segment NCS was conducted to precisely localize CBs in the right median and left ulnar nerves. Although we could not determine the precise location of the CB in the right median nerve due to the difficulty in providing supramaximal stimulation to the median nerve, which runs deep in the right forearm, the CB in the left ulnar nerve was localized to the distal end of the upper arm (Figure B). A blood examination revealed no monoclonal gammopathy, abnormal glucose metabolism, abnormal liver function, abnormal renal function, abnormal thyroid function, or abnormal soluble interleukin-2 levels. Antiganglioside antibodies and antinuclear antibodies were not detected. A cerebrospinal fluid examination yielded normal results. Thus, the patient was diagnosed with MAD-SAM based on the clinical course (23).

Routine peripheral nerve ultrasound revealed the asymmetric enlargement of the cervical nerve roots as well as multifocal peripheral nerve enlargement (Table 2). Notably, additional ultrasonological “inching” studies revealed that, at the site of the CB, the left ulnar nerve became focally enlarged with a loss of the normal fascicular pattern (Figure B). Furthermore, intensive ultrasound assessments of the cranial nerves revealed that the left vagus nerve became focally enlarged with abnormally enlarged hypoechoic fascicles at the level just above the branching point of the left recurrent nerve [CSA, 6.01 mm² (patient) vs. 0.98±0.16 mm² (NCs)] (Figure C), the diameter of the right facial nerve became focally enlarged under the parotid gland [right, diame-

Table 2. Results of Routine Peripheral Nerve Ultrasound at Standardized Points.

Nerve and site	CSA (mm ²)	Nerve roots	CSA (mm ²)
Rt median nerve		Rt C5	5.12 (<7.7)
Wrist	7.23 (<11.9)	Lt C5	6.28 (<7.7)
Forearm	8.45 (<8.6)	Rt C6	<u>13.25</u> (<12.3)
Elbow	12.94 (<13.5)	Lt C6	8.44 (<12.3)
Upper arm	<u>16.31</u> (<11.6)	Rt C7	11.34 (<14.2)
Lt median nerve		Lt C7	10.42 (<14.2)
Wrist	8.17 (<11.9)		
Forearm	6.86 (<8.6)		
Elbow	11.69 (<13.5)		
Upper arm	<u>12.38</u> (<11.6)		
Rt ulnar nerve			
Guyon (Wrist)	5.15 (<6.1)		
Distal sulcus	5.32 (<6.7)		
Elbow	4.13 (<6.2)		
Upper arm	10.41 (<10.5)		
Lt ulnar nerve			
Guyon (Wrist)	4.79 (<6.1)		
Distal sulcus	5.24 (<6.7)		
Elbow	<u>6.89</u> (<6.2)		
Upper arm	9.97 (<10.5)		

Data are expressed with reference values (15, 16). Abnormal values are underlined. Rt: right, Lt: left

ter, 0.50 mm (patient) vs. 0.24±0.04 mm (NCs); left, diameter, 0.21 mm (patient) vs. 0.23±0.02 mm (NCs)] (Figure D), and the hypoglossal, spinal accessory, and optic nerves were normal.

Three days of intravenous methylprednisolone therapy (1,000 mg/day) followed by maintenance therapy with oral prednisolone gradually lead to complete symptomatic remission within one month. In contrast to the improvement of the patient's symptoms, at four months after treatment, NCS still showed CBs in the right median and left ulnar nerves and the focal nerve enlargement observed on ultrasonography showed no improvement.

Discussion

CIDP is a chronic progressive immune-mediated neuropathy characterized by acquired peripheral nerve demyelination (2, 24). CIDP is heterogeneous and consists of several clinical subtypes, including the typical CIDP, distal acquired demyelinating symmetric neuropathy, MADSAM, focal, pure motor, and pure sensory subtypes (23). The subtype classification is clinically important because these clinical subtypes have differing clinical responses to immunomodulatory therapies and prognoses, presumably based on the different underlying pathogenesis (2, 25). However, subtype classification is sometimes difficult; the fact that the diagnosed subtypes change during the clinical course for many CIDP patients clearly indicates how difficult subtype classification can be (26).

In clinical practice, CIDP subtype classification is con-

ducted based on clinical presentations (23). Importantly, the pattern of nerve morphological change is also different among CIDP subtypes and can contribute to CIDP subtype classification, as clearly evidenced by reconstruction magnetic resonance neurography (27). Specifically, typical CIDP patients show root-dominant symmetric hypertrophy, whereas MADSAM patients show multifocal hypertrophy in the nerve trunks (27). Similarly, in peripheral nerve ultrasound studies, typical CIDP tends to show root-dominant symmetric nerve enlargement, while MADSAM shows multifocal enlargement, especially at the site of CBs (6, 28). However, studies describing the investigation of the morphological changes of cranial nerves among CIDP subtypes are scarce in the relevant literature. In this context, our case is important because our case demonstrates that 1) morphological changes similar to those that found in peripheral nerves are likely to occur in many cranial nerves of patients with MADSAM, and 2) if properly and systematically investigated with ultrasound, focal enlargement may be detected in a large proportion of clinically affected cranial nerves in MADSAM. It should be noted that when assessing small nerves like cranial nerves using ultrasonography, the reliability of the measurement is always an issue; thus, future validation studies are warranted. Nevertheless, our finding boosts future investigations to advance the clinical application of cranial nerve ultrasound for CIDP subtype classification.

The authors state that they have no Conflict of Interest (COI).

Acknowledgement

We appreciate Drs. Naoko Uehara and Akihiro Kikuya for their academic support.

References

- Lewis RA, Sumner AJ, Brown MJ, Asbury AK. Multifocal demyelinating neuropathy with persistent conduction block. *Neurology* **32**: 958-964, 1982.
- Kuwabara S, Iose S, Mori M, et al. Different electrophysiological profiles and treatment response in “typical” and “atypical” chronic inflammatory demyelinating polyneuropathy. *J Neurol Neurosurg Psychiatry* **86**: 1054-1059, 2015.
- Rajabally YA, Chavada G. Lewis-sumner syndrome of pure upper-limb onset: diagnostic, prognostic, and therapeutic features. *Muscle Nerve* **39**: 206-220, 2009.
- Shibuya K, Tsuneyama A, Misawa S, et al. Cranial nerve involvement in typical and atypical chronic inflammatory demyelinating polyneuropathies. *Eur J Neurol* **27**: 2658-2661, 2020.
- Goedee HS, Herraets IJT, Visser LH, et al. Nerve ultrasound can identify treatment-responsive chronic neuropathies without electrodiagnostic features of demyelination. *Muscle Nerve* **60**: 415-419, 2019.
- Décard BF, Pham M, Grimm A. Ultrasound and MRI of nerves for monitoring disease activity and treatment effects in chronic dysimmune neuropathies - Current concepts and future directions. *Clin Neurophysiol* **129**: 155-167, 2018.
- Shibuya K, Yoshida T, Misawa S, et al. Hidden Charcot-Marie-Tooth 1A as revealed by peripheral nerve imaging. *Intern Med* **58**: 3157-3161, 2019.
- Granata G, Pazzaglia C, Calandro P, et al. Ultrasound visualization of nerve morphological alteration at the site of conduction block. *Muscle Nerve* **40**: 1068-1070, 2009.
- Scheidl E, Böhm J, Simó M, et al. Ultrasonography of MADSAM neuropathy: focal nerve enlargements at sites of existing and resolved conduction blocks. *Neuromuscul Disord* **22**: 627-631, 2012.
- Simon NG, Kiernan MC. Precise correlation between structural and electrophysiological disturbances in MADSAM neuropathy. *Neuromuscul Disord* **25**: 904-907, 2015.
- Tanaka K, Ota N, Harada Y, Wada I, Suenaga T. Normalization of sonographical multifocal nerve enlargements in a MADSAM patient following a good clinical response to intravenous immunoglobulin. *Neuromuscul Disord* **26**: 619-623, 2016.
- Grimm A, Thomaser A-L, Peters N, Fuhr P. Neurological picture. Vagal hypertrophy in immune-mediated neuropathy visualised with high-resolution ultrasound (HR-US). *J Neurol Neurosurg Psychiatry* **86**: 1277-1278, 2015.
- Kimura J. *Electrodiagnosis in Diseases of Nerve and Muscle: Principles and Practice*. 3rd ed. Oxford University Press, New York, 2001.
- Iose S, Kuwabara S, Kokubun N, et al. Utility of the distal compound muscle action potential duration for diagnosis of demyelinating neuropathies. *J Peripher Nerv Syst* **14**: 151-158, 2009.
- Won SJ, Kim B-J, Park KS, Kim SH, Yoon JS. Measurement of cross-sectional area of cervical roots and brachial plexus trunks. *Muscle Nerve* **46**: 711-716, 2012.
- Sugimoto T, Ochi K, Hosomi N, et al. Ultrasonographic reference sizes of the median and ulnar nerves and the cervical nerve roots in healthy Japanese adults. *Ultrasound Med Biol* **39**: 1560-1570, 2013.
- Tawfik EA, Walker FO, Cartwright MS. Neuromuscular ultrasound of cranial nerves. *J Clin Neurol* **11**: 109-121, 2015.
- Tawfik EA, Walker FO, Cartwright MS. A pilot study of diagnostic Neuromuscular Ultrasound in Bell's Palsy. *J Neuroimaging* **25**: 564-570, 2015.
- Meng S, Reissig LF, Tzou C-H, Meng K, Grisold W, Weninger W. Ultrasound of the hypoglossal nerve in the neck: visualization and initial clinical experience with patients. *AJNR Am J Neuroradiol* **37**: 354-359, 2016.
- Tsukita K, Taguchi T, Sakamaki-Tsukita H, Tanaka K, Suenaga T. The vagus nerve becomes smaller in patients with Parkinson's disease: a preliminary cross-sectional study using ultrasonography. *Parkinsonism Relat Disord* **55**: 148-149, 2018.
- Tsukita K, Sakamaki-Tsukita H, Tanaka K, Suenaga T, Takahashi R. Value of in vivo α -synuclein deposits in Parkinson's disease: a systematic review and meta-analysis. *Mov Disord* **34**: 1452-1463, 2019.
- Bromberg MB, Albers JW. Patterns of sensory nerve conduction abnormalities in demyelinating and axonal peripheral nerve disorders. *Muscle Nerve* **16**: 262-266, 1993.
- Van den Bergh PYK, Hadden RDM, Bouche P, et al. European Federation of Neurological Societies/Peripheral Nerve Society guideline on management of chronic inflammatory demyelinating polyradiculoneuropathy: report of a joint task force of the European Federation of Neurological Societies and the Peripheral Nerve Society - first revision. *Eur J Neurol* **17**: 356-363, 2010.
- Koike H, Nishi R, Ikeda S, et al. Restoration of a conduction block after the long-term treatment of CIDP with anti-neurofascin 155 antibodies: follow-up of a case over 23 years. *Intern Med* **57**: 2061-2066, 2018.
- Ikeda S, Koike H, Nishi R, et al. Clinicopathological characteristics of subtypes of chronic inflammatory demyelinating polyradiculoneuropathy. *J Neurol Neurosurg Psychiatry* **90**: 988-996, 2019.
- Doneddu PE, Cocito D, Manganelli F, et al. Atypical CIDP: diagnostic criteria, progression and treatment response. Data from the Italian CIDP Database. *J Neurol Neurosurg Psychiatry* **90**: 125-132, 2019.
- Shibuya K, Sugiyama A, Ito S, et al. Reconstruction magnetic resonance neurography in chronic inflammatory demyelinating polyneuropathy. *Ann Neurol* **77**: 333-337, 2015.
- Gasparotti R, Padua L, Briani C, Lauria G. New technologies for the assessment of neuropathies. *Nat Rev Neurol* **13**: 203-216, 2017.

The Internal Medicine is an Open Access journal distributed under the Creative Commons Attribution-NonCommercial-NoDerivatives 4.0 International License. To view the details of this license, please visit (<https://creativecommons.org/licenses/by-nc-nd/4.0/>).